Accessing Sulfonamides via Formal SO_2 Insertion into C–N Bonds

Myojeong Kim,[1] Carys E. Obertone,[1] Christopher B. Kelly,[2,*] Christopher A. Reiher,[3,*] Cristina Grosanu,[4] James C. Robertson,[5] and Mark D. Levin[1,*]

[1]Department of Chemistry, University of Chicago, Chicago, Illinois 60637, United States

[2]Discovery Process Research, Johnson & Johnson Innovative Medicine, Spring House, Pennsylvania 19477, United States

[3]Parallel Medicinal Chemistry, Johnson & Johnson Innovative Medicine, Spring House, Pennsylvania 19477, United States

[4]High-Throughput Purification, Johnson & Johnson Innovative Medicine, Spring House, Pennsylvania 19477, United States

[5]In Silico Discovery, Johnson & Johnson Innovative Medicine, Spring House, Pennsylvania 19477, United States

Supporting Information Placeholder

ABSTRACT: Functional group interconversions of abundant substructures that accommodate the often-complex molecular architectures seen in pharmaceuticals are particularly sought after by medicinal chemists as a means to enable both lead optimization and library diversification. Here, we report a conceptually new strategy that enables net SO_2-insertion into the C–N bond of primary amines, enabling the direct synthesis of primary sulfonamides without pre-activation and effectively inverting the nitrogen's properties (acidity, hydrogen bonding, etc.). The key to realizing this overall transformation is the implementation of an anomeric amide as a dual-function reagent which both serves to cleave the initial C–N bond and deliver a nitrogen atom to the product after SO_2 incorporation. The process tolerates a wide array of functionalities and can be run in an automated fashion thus allowing libraries of amines to be viable progenitors to highly desirable sulfonamides. Mechanistic studies support an isodiazene radical chain mechanism that generates an intermediate sulfinate which reacts with the anomeric amide to forge the S–N bond. As a proof of concept, our protocol was used to conduct a high-throughput library diversification campaign, was applied to the synthesis and modification of approved active pharmaceutical ingredients and was used to enable a net CO-to-SO_2 "isosteric replacement" approach. Conceptually, this successful translation of a reagent originally developed for atom deletion into a protocol for atom insertion has important implications for skeletal editing.

Amine-containing functional groups (-NH_2) are privileged in medicinal chemistry, serving as versatile pharmacophore elements.[1,2] The structural diversity, pharmacological activity, and synthetic versatility of these handles can be tuned by the nitrogen atom's immediate bonding environment (i.e. the vast difference in chemical reactivity and properties of primary amines[3–5], amides[6,7], and sulfonamides[8–10]). However, interconversion between these categories of nitrogenous functional group is non-trivial and often requires tailored syntheses to accommodate the unique reactivities of

each subclass. Considering that primary amines comprise a significant fraction of building block libraries in the drug discovery sector, a reaction that connects the sheer diversity of such libraries to other NH_2 subclasses has transformative potential. In particular, the sulfonamide group frequently appears in pharmaceutical compounds[11–13] over a wide range of indications (e.g. antibiotics, diuretics, and anti-cancer agents), despite being relatively uncommon in nature (see Fig 1a, left). Unfortunately, the disparity in abundance between these sulfonyl species and primary amines in commercial libraries[14] hinders their assessment in screening campaigns. To put this in perspective, mining of the Mcule database (commonly used as a starting point for virtual screening) lists ~6,400 purchasable primary sulfonamide derivatives whereas over 40,000 primary amines are available from commercial vendors[15]. This asymmetry underscores a clear synthetic need for NH_2 to SO_2NH_2 interconversion. Beyond charting new chemical space, such direct conversions could also expedite the optimization of lead compounds. As an emblematic example, a recent lead optimization campaign of an I_{Kur} enzyme inhibitor examined a range of such functionality on a flanking heteroaromatic ring, ultimately finding that a primary sulfonamide was the ideal analog[10] (Fig 1a, right), particularly due to its ability to reduce blood-brain barrier penetration. To identify this lead, independent (non-convergent) syntheses of the amine, primary amide, and sulfonamide amide analogs were executed, presumably resulting in delays in generating SAR data.

Despite notable recent advances for primary sulfonamide synthesis from carboxylic acids[16,17] and alcohols[18], approaches using primary amines as starting points for direct sulfonamide construction remain elusive and thus practionners are forced into regimes based on manipulations at sulfur. To overcome this clear gap in the current art, we became interested in inserting SO_2 directly into the C–N bond of primary amines (Fig 1b, left top). However, the C–N bonds of primary amines are typically kinetically inert (low nucleofugality), and direct activation is challenging due to competing nucleophilicity and susceptibility to oxidation-induced decomposition[19–23]. These challenges have historically necessitated pre-functionalization strategies including Katrizky-type pyridiniums, isonitriles, diazoniums, or redox-active imines[14,20–22,24–28]. In contrast, electrophilic anomeric amide reagent **1**[29,30], investigated by our group[31,32] and others[33], is a rare exception, as it enables the generation of free radicals from primary amines *without pre-activation* (Fig 1b, right). The challenge in this activation manifold is two-fold – a successful approach must (i) outcompete incipient reduction of the radical by the isodiazene intermediate while (ii) maintaining a productive radical chain process by engaging the isodiazene after productive radical trapping. As such, to date, only a limited set of radical trapping agents have successfully been leveraged in combination with **1**.[32]

Our investigations were guided by several reactivity principles. First, sulfur dioxide is known to rapidly trap carbon-centered radicals, suggesting that the deleterious hydrogen atom transfer (HAT) by C-centered radicals would be effectively outcompeted[34,35]. Although the fate of the sulfonyl radical is dictated by many factors (structure, solvent, etc.), it is well established that it can engage in HAT processes, yielding sulfinic acids (reactive species which are viable

nucleophiles for substitution-processes). In the presence of reagents such as O-(mesitylsulfonyl)hydroxylamine (MSH) and hydroxylamine-O-sulfonic acid (HOSA), sulfinates are known to undergo electrophilic amination affording primary sulfonamides.[18,25,36] In an equivalent fashion, we hypothesized that the anomeric amide, with its strong electrophilic nature, could act in such a capacity thus serving as to deaminate, sulfonylate, and re-aminate all in one concise operation (Fig 1b, left bottom). Herein we report the realization of this approach allowing for the net SO_2 insertion between the C–N bond of primary amines by the action of anomeric amide reagent **1** (Fig 1c).

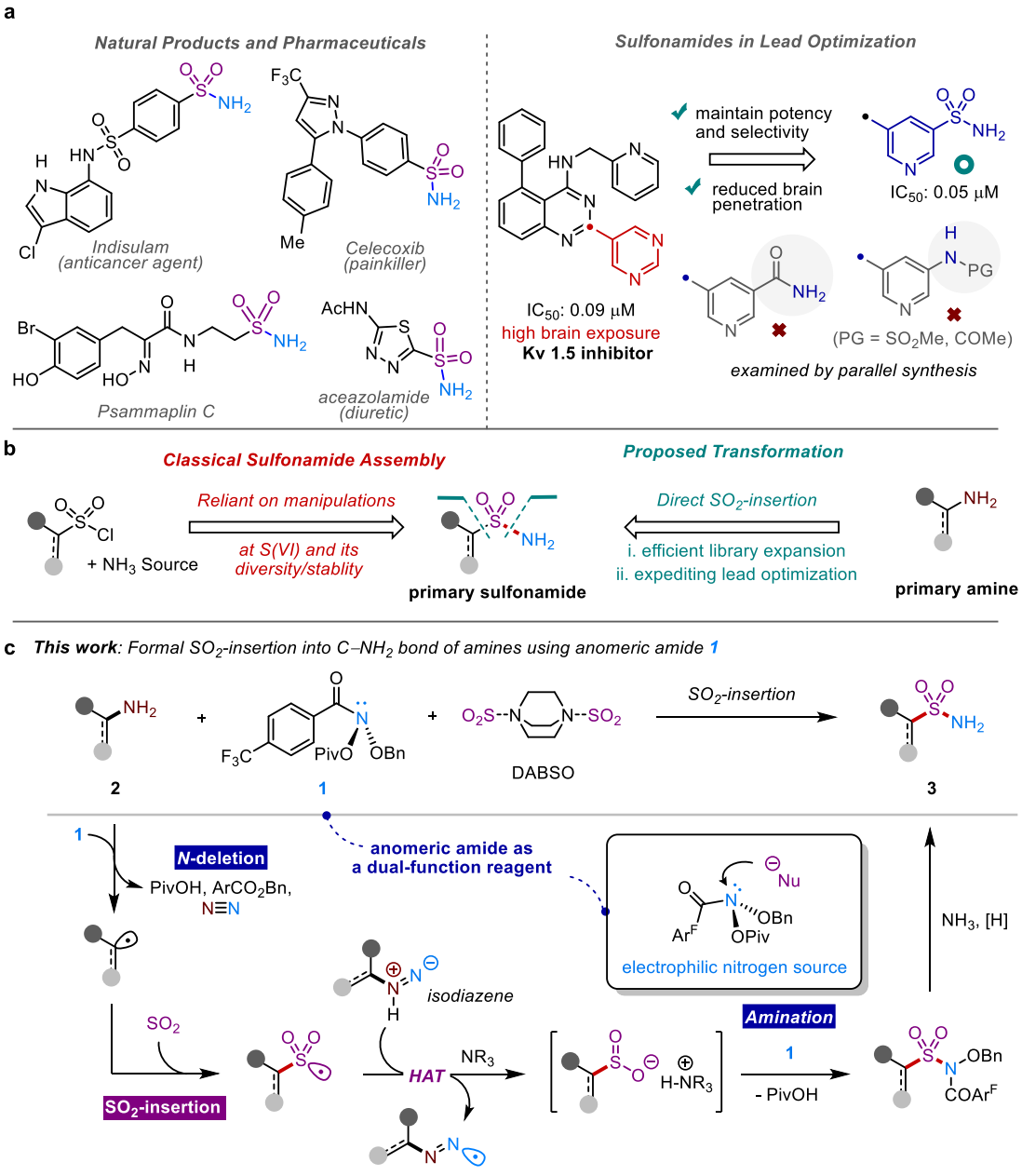

Fig. 1: Overview of this study. a, Primary sulfonamides with therapeutic potential. **b,** Our goal and strategy for underdeveloped direct SO_2-insertion. **c,** This work.

Results and Discussion

Reaction Discovery and Optimization Initial studies centered on identification of an SO_2 source amenable for trapping of carbon-centered radicals generated by reagent **1**. Although preliminary studies using 4-amino-1-Cbz-piperidine (**2a**) and anomeric amide **1** with various SO_2 sources validated our mechanistic hypothesis regarding the dual-function reactivity of **1**, a mixture of sulfonamide derivatives (**4a**, **4a′**) and the deaminated alkane (**5a**) in varying product ratios (Fig 2) were obtained. Although direct deamination exhibited high productivity in the absence of SO_2 (entry 1, **5a**, 76%), indicating an efficient deaminative radical generation, we observed lower conversion of the amine when directly employing a solution of SO_2 in THF (entry 2, 32% and 14%, each). We attribute this inferior conversion to the formation of charge-transfer complexes between the amine and SO_2, which inhibits the reaction with **1**. To prevent this, we evaluated a wide range of organic and inorganic bases (see SI for details). Among them, Et_3N was found to dramatically improve yield and predominantly give desired products (entry 3, 69%). Furthermore, employing a "slow-release" SO_2 surrogate[37] such as DABSO (1,4-diazabicyclo[2.2.2]octane bis(sulfur dioxide) adduct) was found to generally increase the conversion of **2** into products **4** and **4′** (entry 4 and see the SI). Additionally, other commercially available SO_2 surrogates, such as TIMSO (sulfur dioxide 1-methylpyrrolidine adduct), exhibited similar but lower efficiency, while metabisulfite (i.e. $Na_2S_2O_5$ and $K_2S_2O_5$) did not provide any sulfonamide (entries 6, 7, and see the SI). Lastly, we also found that using increased amounts of DABSO (3 equiv) completely inhibited the production of **5a** but resulted in lower yields overall, suggesting that using 2 equivalents is optimal (entries 4 vs. 7). Control experiments employing other electrophilic aminating reagents (e.g. HOSA and $PivONH_3OTf$) in combination with anomeric amide **1** were not productive, resulting in low yields of protodeamination product **5a** (20% and 28%, respectively), with no sulfonamide products detected (see SI for details).

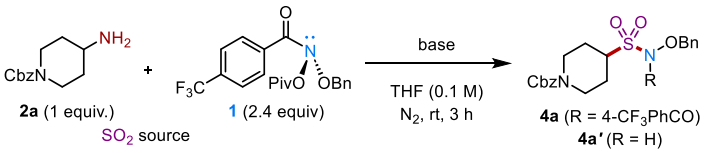

entry	SO_2 source (equiv)	base (equiv)	**4a** + **4a′** (**4a** / **4a′**) (%)	**5a** (%)
1	-	-	-	76
2	SO_2 in THF (4.0)	-	32 (26/6)	14
3	SO_2 in THF (4.0)	Et_3N (2.9)	69 (61/8)	2
4	DABSO (2.0)	Et_3N (2.9)	**75 (66/9)**	1
5	TIMSO (4.0)	Et_3N (2.9)	62 (53/9)	0
6	$Na_2S_2O_5$ (4.0)	Et_3N (2.9)	0	70
7	DABSO (3.0)	Et_3N (2.9)	66 (58/8)	0

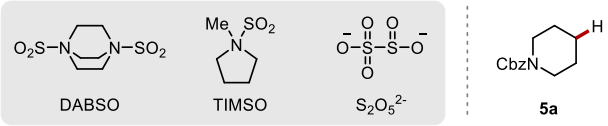

Fig. 2: Select optimization data for the SO_2 insertion process

To readily access primary sulfonamide of type **3**, **4** (and any residual 4′) could be subjected to a known debenzoylation protocol (aq. NH_4OH) followed by reductive N–O cleavage with catalytic $[RuCl_2(p\text{-cymene})]_2$[38] (see SI for details). This overall sequence is accomplished in a single pot without isolation of any intermediates and with only a single purification, thus effectively delivering the desired SO_2 insertion process.

Substrate Scope Studies. With viable conditions for SO_2 insertion defined, we sought to understand the generality of this newly established method (Table 1). Indeed, both α-primary and α-secondary aliphatic amines were competent substrates, affording a range of structurally diverse sulfonamides (**3b**-**3k**). Of particular note were medicinally relevant species such as bioisosteric[39] oxo-bicyclohexane **3f** and bicyclopentyl species **3l** as well as the ability to generate unnatural amino acids rapidly (e.g. lysine-derived **3g**). Notably, our reaction conditions were compatible with an array of functional groups commonly employed in screening campaigns including N-carbamates[40] (**3g**) and basic nitrogen heterocycles[41] (**3l**). Stereochemical integrity was maintained in morpholine derivative **3d** and lysine derivative **3g** (e.e >99% and >99%, respectively). To explore the broad applicability of the net SO_2 insertion reaction, we modified biorelevant amines, successfully applying it to medicinally active agents like rimantadine, leelamine, and primaquine, yielding their respective sulfonamide products (**3m**, **3n**, and **3o**). Next, we investigated the scope of aromatic amines with varying electronic and steric demands of aryl substituents. Under slightly modified reaction conditions (MeCN as the solvent, no added base, and 45 °C reaction temperature), the reaction was successful with anilines bearing a broad range of functional groups (**3p**-**3y**), including a range of disubstituted and heteroaromatic anilines (indole, naphthol, and dibenzofuran), ranging from 50% to 79% yield (**3t**, **3u**, and **3v**) and aminoglutethimide (**3y**) in 42% yield.

High-Throughput Library Evaluation. To better understand how this method may be used to tap into the diversity of amine screening libraries to generate wholly new sulfonamide fragments, a parallel medicinal chemistry (PMC) workflow that heavily leveraged high throughput technologies (robotics for dosing, workup, and purification) was designed. In terms of chemical matter, a diverse array of amines was selected to strategically cover diverse, pharmaceutically-relevant structural space (visualized in the TSNE plot, Fig. S1) while simultaneously ensuring that key matched molecular pairs were represented.[42–44] The selection process prioritized pharmaceutically significant motifs, encompassing saturated and unsaturated heterocycles, as well as hydrogen bond donors and acceptors. In total, 84 solid dispenses of DABSO into vials containing pre-weighed amine substrates and >700 liquid transfers were automated over the course of reaction set-up, work-up, and analysis, in a process that took a mere 24 h to execute end-to-end. To better enable rapid purification in this model workflow and also further understand the potential impurities generated across an array of substrates, we elected to halt the synthetic sequence just prior to reductive N–O cleavage.

Table 1: Substrate Scope.

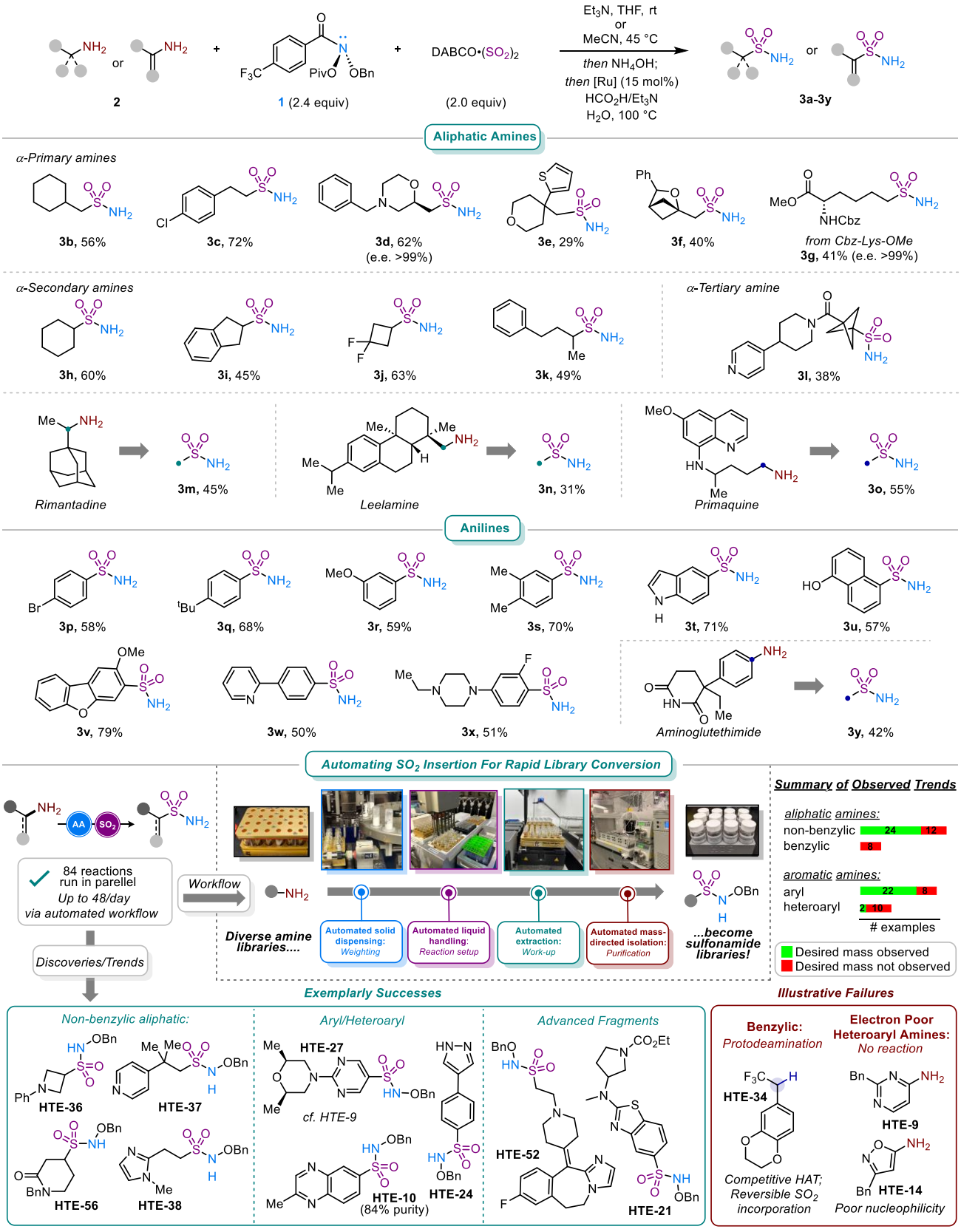

Reaction conditions for aliphatic amines: **2** (0.2 mmol, 1.0 equiv), **1** (2.4 equiv), DABSO (2.0 equiv), and Et_3N (2.9 equiv) were stirred in THF (0.1 M) at rt under N_2 for 3 h. Reaction conditions for anilines: **2** (0.2 mmol, 1.0 equiv), **1** (2.4 equiv), DABSO (2.0 equiv) were stirred in CH_3CN (0.1 M) at 45 °C under N_2 for 20 h. After reaction completion, aq. NH_4OH (0.1 mL) was added and stirred at rt for 2 h, then solvents were evaporated. $[Ru(p\text{-cymene})_2Cl_2]_2$ (15 mol%) was added to the crude mixture, which was then stirred in HCOOH/Et_3N 5/2 : H_2O (1:1, 0.2 M) at 100 °C for 2–20 h. For details on automated workflow, see SI.

The summarized results are presented in Table 1 (see SI for details). The overall workflow allowed for >5 mg of product to be isolated in many cases in high purity. In terms of chemical trends observed, aliphatic and aryl amines generally underwent productive SO_2-insertion with a higher success rate than their heteroaryl congeners. A wide range of functionalities including pendant 5- and 6-membered heterocycles (**HTE-38** and **HTE-37**), as well as basic amines (**HTE-52**) were tolerated. **HTE-37** is also of particular note as it is highly sterically congested. α-Cyclic benzyloxy sulfonamides were also accessible, exemplified by azetidine **HTE-36** and lactam **HTE-56**. Benzylic substrates failed to undergo SO_2-insertion presumably due to reversibility of SO_2 capture[45] Instead, protodeamination (**HTE-34**), elimination, and dimerization processes were observed (See SI for details). However, electronic factors did not always guarantee failure: an inductively withdrawn β-amino substrate (**HTE-52**) was quite successful. An array of aniline derivatives successfully underwent SO_2-insertion, including those fused to an electron deficient ring (**HTE-10**) and in the presence of an unprotected pyrazole (**HTE-24**). In contrast, the heteroaryl amines evaluated were generally found incongruent with the SO_2 insertion process, likely due to low nucleophilicity, although a strong electron-donating substituent can counteract this effect (**HTE-27**). Finally, **HTE-21** and **HTE-52** further illustrate the utility of this method in late-stage functionalization of molecules with complex, functional group rich architectures.

Synthetic Utility. With the success of the insertion process across a range of disparate primary amines and the capability to execute this workflow in an automated fashion demonstrated, we next sought to test the bounds of this protocol for influencing drug design. We thus subjected complex amine-containing drug, Crenolanib[46,47] (RTK inhibitor, targeted therapy for specific cancers) to our SO_2 insertion protocol. The logic behind selecting this molecule was twofold: 1) it represents a hypothetical late-lead optimization candidate that may "need" alteration to accommodate challenges that associated with a free primary amine and 2) a co-crystal of this species with its target is known in the literature, and thus the overall influence on the binding pose after insertion could be easily evaluated. In the event, Crenolanib underwent insertion with ease, affording the corresponding sulfonamide product **3z** in synthetically and biochemically viable yield. To evaluate the effect of this change on the binding, Crenolanib, and its newly synthesized sulfonamide analogue **3z** were investigated with docking simulations.[48] The zoomed in view (Fig 3a) shows that self-docking of Crenolanib to PDGFR (PDB ID: 6JOJ) agrees with the X-ray structure. Docking of the sulfonamide analog **3z** (following the same docking procedure) shows nearly complete overlap with the shared substructure atoms of Crenolanib, with a potential for improved interaction between the sulfonamide moiety and the nearby Asp681 residue on the receptor. As a further extension of our method, we examined the conversion of amides to sulfonamides, a bioisosteric replacement of a carbonyl for a sulfonyl[49,50] (CO to SO_2) (Fig 3b). This was accomplished by taking advantage of a PIFA-mediated Hofmann reaction[51] to first convert the amide to an amine, followed by the application of insertion method described here. We demonstrated this on 4-piperidinecarboxamide derivative (**6**, widely used motif in drug discovery), forming the corresponding sulfonamide **3a** in

53% overall yield. This is a direct analog of a medicinal chemistry strategy outlined in Fig. 1a above, which is often employed because of the effects on pK_a[52] and geometry (17.5 vs. 25.5, DMSO; planar vs. pyramidal NH_2). Lastly, we capitalized on the data generated by our PMC efforts to enable rapid construction of an API (Fig 3c). Pazopanib, an FDA-approved tyrosine kinase inhibitor, was synthesized from two commercially available building blocks in a total yield of 46% (**3aa**).

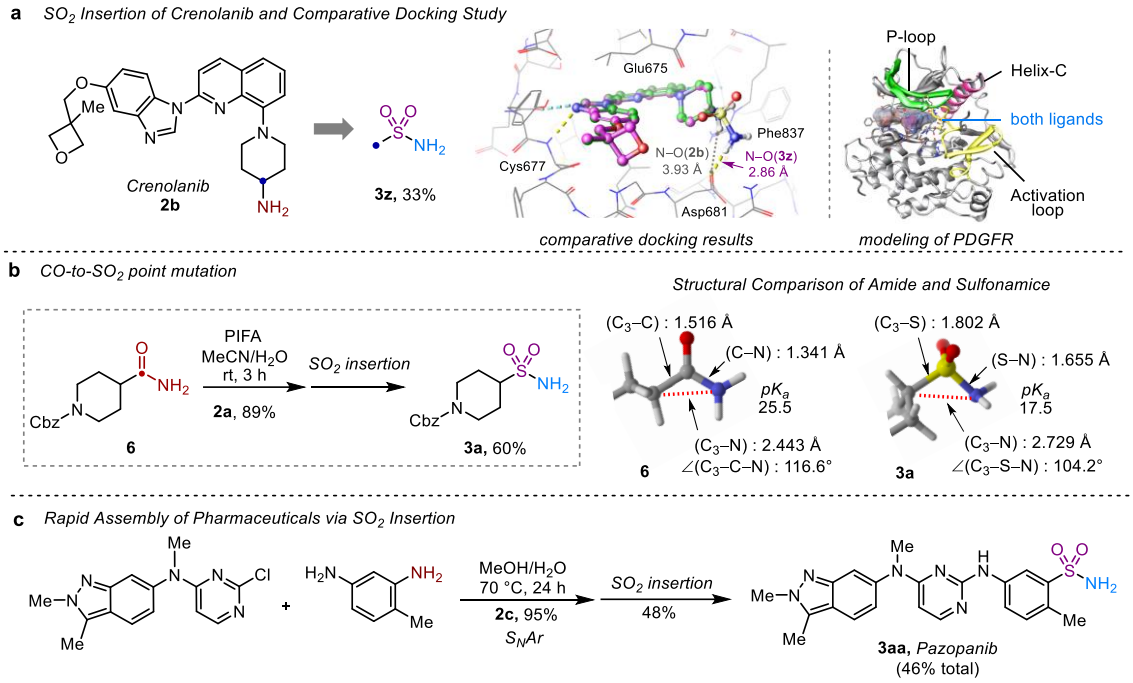

Fig 3: Synthetic utility. a. Modification of Crenolanib and comparative docking study to PDGFR. The full kinase domain is also shown with key structural motifs highlighted. **b.** Synthesis of primary sulfonamide from amide, pK_a prediction, and theoretical geometry comparison. **c.** Synthesis of tyrosine kinase inhibitor Pazopanib via SO_2 insertion.

Mechanistic Experiments. To better understand the mechanistic underpinnings of the SO_2 insertion reaction described here, a series of experiments were performed to elucidate the reaction mechanism (Fig 4). Variation of the loading of DABSO resulted in a corresponding change in the yield of **4a** and **4a′** (Ar^F = 4-CF_3Ph) – while the overall mass balance was unchanged, the ratio of protodeamination byproduct **5a** increased as the loading of DABSO decreased (Fig 4a), indicating that these two pathways arise via competitive mechanisms that diverge from a common intermediate (a carbon-centered radical). In further support of this, we conducted a radical clock experiment using aromatic amine **2d** under standard reaction conditions and obtained cyclized products exclusively (Fig 4b). To demonstrate the viability of sulfinates to engage reagent **1** in substitution at nitrogen, we subjected triethylammonium cyclohexylsulfinate (**7**) to anomeric amide **1**. Sulfonamides **4b** and **4b′** were observed in 92% total yield, supporting the intermediacy of sulfinates. Further, to confirm that the source of nitrogen in the observed products is indeed from reagent **1**, we subjected amine **2e** to our reaction conditions using isotopically labeled ^{15N}**1.** As anticipated, ^{15N}**4c′** was exclusively obtained (40% yield, >99% ^{15}N),

supporting that the nitrogen of the product arises from the anomeric amide (Fig 4d). Lastly, a trapping experiment using *N*-sulfinyl tritylamine (TrNSO)[17] affords the corresponding sulfinyl amine **8** without subsequent reaction with the anomeric amide (Fig 4e), further supporting the intermediacy of the sulfinate under the parent conditions.

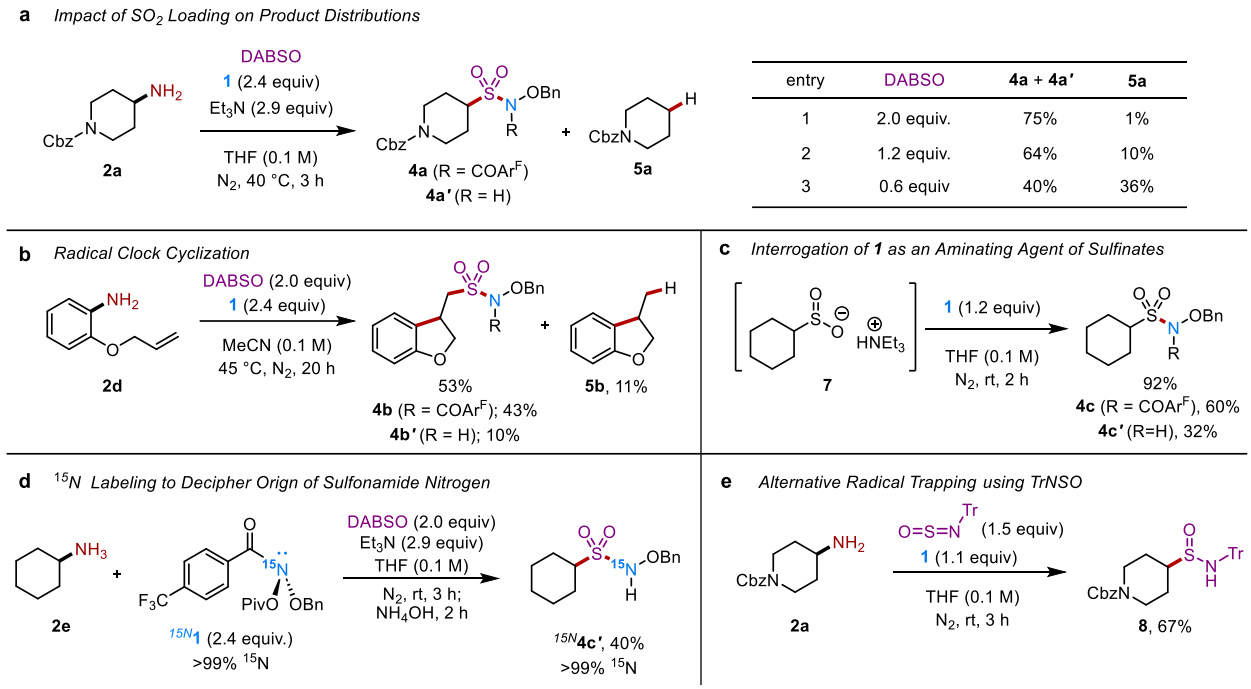

Fig 4: Mechanistic investigations.

Computational Analysis. Based on these experimental mechanistic studies and the prior art, a plausible mechanism can be constructed involving a sulfinate intermediate (**Fig 5a**). As previously established, formation of isodiazene ***I*** from the primary amine substrate and anomeric amide **1** proceeds rapidly, leading to the generation of alkyl radical **A** and diazenyl radical **B**. C-centered radical **A** is successively trapped by SO_2, forming the radical **C**. This sulfonyl radical engages isodiazine species ***I*** in HAT, leading to sulfinic acid **D.** Under the optimized reaction conditions, this acidic species undergoes facile deprotonation to generate an ammonium sulfinate salt. The radical chain is sustained by subsequent homolysis of diazenyl radical **E**, extruding dinitrogen (N_2) gas and regenerating alkyl radical **A**. Finally, reaction of the ammonium salt of **D** with anomeric amide **1** yields product **4**.

To better understand the observed selectivity in this transformation, we conducted computational studies, focusing on the fate of the open-shell intermediates along the reaction pathway. Density functional theory (DFT) calculations at the DLPNO/CCSD-(T)/def2-TZVPP//(U)-ωB97XD/6-31+G(d,p)-SMD(THF) level of theory[35,53,54], were carried out to investigate the energetic barriers between the two competitive HAT pathways of the isodiazene (sulfinyl radical vs. alkyl radical) and their interplay with the barrier for homolytic attack on SO_2 by C-centered radicals (and its relative reversibility). Initial examination of HAT using ethyl isodiazene ^{Et}***I*** with ethyl radical ^{Et}**A**, resulted in a barrier of $\Delta G^{\ddagger}$ = 9.8 kcal mol^{-1} (red lines in Fig 5b). Alternatively, attack on SO_2 is barrierless and greatly favors formation of sulfonyl

radical ^{Et}**C**.[34,35,52] From there, the barrier for HAT between sulfonyl radical ^{Et}**C** and ethyl isodiazene ^{Et}***I*** to produce sulfinic acid ^{Et}**D** and radical ^{Et}**E** was found to be 6.6 kcal mol^{-1} relative to **D**, or 1.9 kcal mol^{-1} relative to **A** (black lines in Fig 5b). This 3.2 kcal/mol difference indicates that ^{Et}***I*** reacts preferentially with ^{Et}**C**, while the absolute difference between the putative HAT transition states shows a drastic difference of 7.9 kcal mol^{-1} thus suggesting that success here is primarily based on differences in HAT barriers between S- and C-centered radicals with the isodiazine intermediate.

Further examination of geometry of sulfonyl radical based HAT (**C-TS-D**) can be seen in the inset of Fig 5b and illustrates that the lowest energy structure of **C-TS-D** is one in which both oxygen atoms of the sulfinyl radical moiety interact with the N–H bond of isodiazene. The N–H bond distance is calculated to be 1.11 Å and both O–H bonds are computed as about 1.8 Å (1.77 Å and 1.81 Å). Alternative transition state **TS-I**, involving the perpendicular approach of isodiazene, is observed to exhibit a slightly higher energy (ΔG = 1.0 kcal/mol). In contrast, alternate **TS-II**, with a single, dominant N–H–O interaction[35], has a barrier of $\Delta G^{\ddagger}$ = 24.2 kcal/mol, which is 17.6 kcal/mol higher than the kinetic barrier of **C-TS-D**. This transition state is much earlier than **C-TS-D**, as evidenced by a significantly shorter N–H bond distance of 1.05 Å and a significantly longer O–H bond distance of 1.94 Å. Based on these computations, we infer that interactions of isodiazene hydrogen with both oxygen atoms might play a key role in stabilizing the transition state (see SI for details).

Conclusion

In summary, we have developed a direct SO_2 insertion into the C–N bond of primary amines driven by the synergy between an anomeric amide reagent and SO_2. The dual role of the anomeric amide as a homolytic deaminating agent (cleaving the N–C bond) and as an effective electrophilic nitrogen trap (forging the S–N bond) allows for seamless assembly of sulfonamides under the conditions described here. This late-stage amenable approach affords the end-user the ability to tactically modify biologically relevant amines into sulfonamides in both a singleton (thus permitting point mutations on complex targets) or in parallel automated mode. The latter may be used to construct diverse arrays of sulfonamides whose currently mapped chemical space is only a fraction of their amine progenitors. Mechanistic data derived from both experiment and calculations, support the intermediacy of a sulfonyl radical which outcompetes C-centered radicals in HAT events involving isodiazines. More broadly, the implementation of a reagent originally designed for atom deletion to instead promote an overall atom insertion represents a generalizable approach that may have significant applications in skeletal editing.

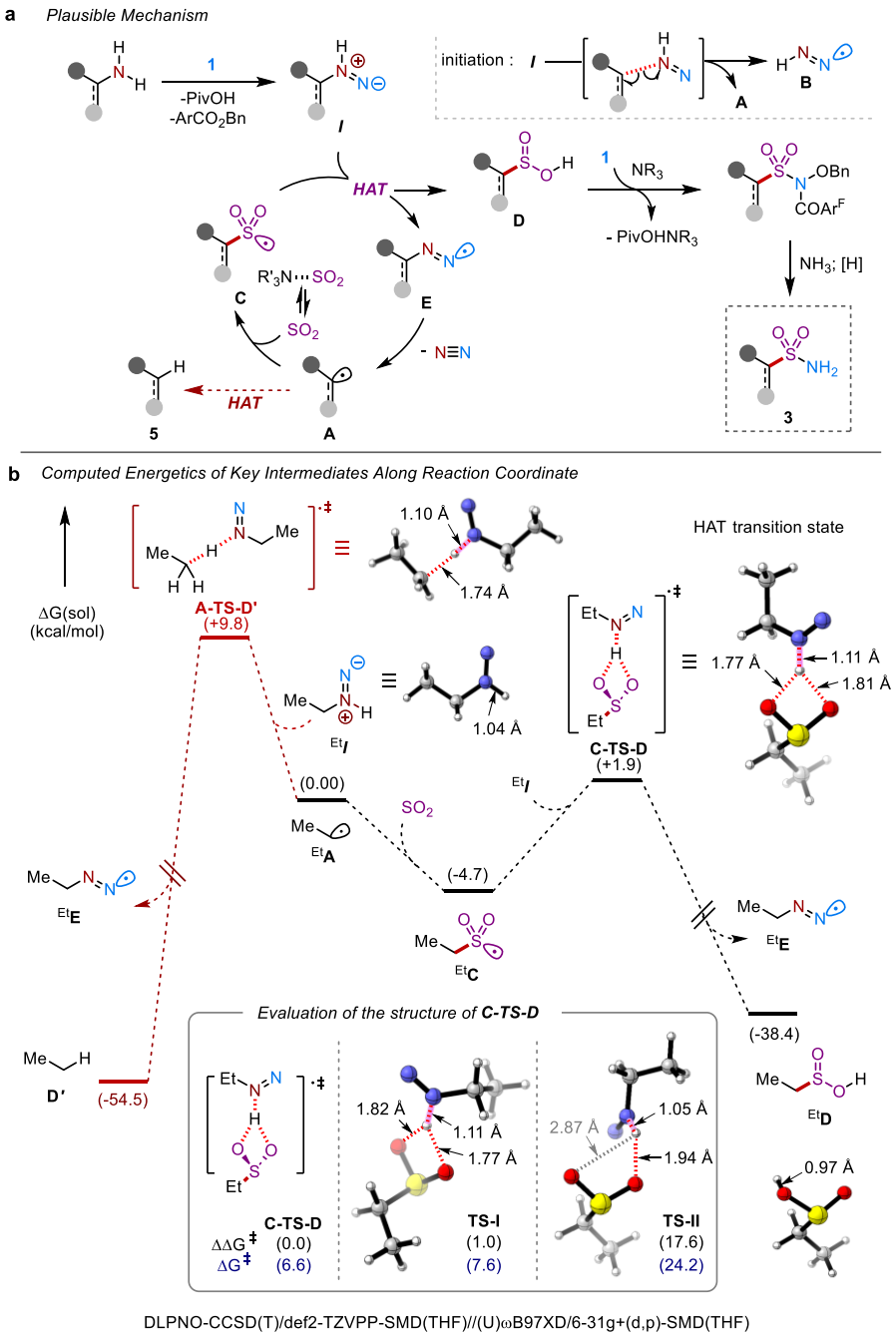

Fig 5: Mechanism and DFT Calculations. a. Proposed reaction mechanism. **b.** DFT investigation of competitive SO_2 trapping and HAT pathways with computed energetic barriers.

AUTHOR INFORMATION

Corresponding Authors

*E-mail: marklevin@uchicago.edu

ckelly5@its.jnj.com

creiher@its.jnj.com

ORCID

Myojeong Kim: 0000-0002-3852-3566

Carys E. Obertone: 0009-0009-8904-1450

Christopher B. Kelly: 0000-0002-5530-8606

Christopher A. Reiher: 0000-0002-6171-3480

James C. Robertson: 0000-0002-9529-5950

Mark D. Levin: 0000-0002-4461-363X

ACKNOWLEDGMENT

M.K. thanks the National Research Fondation of Korea (Grant Number RS-2023-00237898) for a postdoctoral fellowship. The research reported in this work was supported by a National Science Foundation CAREER Award (2235826) and by Johnson and Johnson Innovative Medicine. We also thank Dr. Scott Wolkenberg (Johnson & Johnson) for useful discussions and feedback.

Competing interests

The authors declare no competing interests.

REFERENCES

1. Ertl, P., Altmann, E. & McKenna, J. M. The Most Common Functional Groups in Bioactive Molecules and How Their Popularity Has Evolved over Time. *J. Med. Chem.* **63**, 8408–8418 (2020).
2. Bhutani, P. *et al.* U.S. FDA Approved Drugs from 2015–June 2020: A Perspective. *J. Med. Chem.* **64**, 2339–2381 (2021).
3. Younis, Y. *et al.* Structure–Activity-Relationship Studies around the 2-Amino Group and Pyridine Core of Antimalarial 3,5-Diarylaminopyridines Lead to a Novel Series of Pyrazine Analogues with Oral in Vivo Activity. *J. Med. Chem.* **56**, 8860–8871 (2013).
4. Zhang, S. *et al.* A small-molecule activation mechanism that directly opens the KCNQ2 channel. *Nat. Chem. Biol.* **20**, 847–856 (2024).
5. Cohen, L. J. *et al.* Commensal bacteria make GPCR ligands that mimic human signalling molecules. *Nature* **549**, 48–53 (2017).
6. Velilla, J. A. *et al.* Structural basis of colibactin activation by the ClbP peptidase. *Nat. Chem. Biol.* **19**, 151–158 (2023).
7. Flinspach, M. L. *et al.* Structural basis for dipeptide amide isoform-selective inhibition of neuronal nitric oxide synthase. *Nat. Struct. Mol. Biol.* **11**, 54–59 (2004).
8. Lopez, M. *et al.* S-Glycosyl Primary Sulfonamides−A New Structural Class for Selective Inhibition of Cancer-Associated Carbonic Anhydrases. *J. Med. Chem.* **52**, 6421–6432 (2009).
9. Uehara, T. *et al.* Selective degradation of splicing factor CAPERα by anticancer sulfonamides. *Nat. Chem. Biol.* **13**, 675–680 (2017).
10. Gunaga, P. *et al.* Selective IKur Inhibitors for the Potential Treatment of Atrial Fibrillation: Optimization of the Phenyl Quinazoline Series Leading to Clinical Candidate 5-[5-Phenyl-4-(pyridin-2-ylmethylamino)quinazolin-2-yl]pyridine-3-sulfonamide. *J. Med. Chem.* **60**, 3795–3803 (2017).
11. Ovung, A. & Bhattacharyya, J. Sulfonamide drugs: structure, antibacterial property, toxicity, and biophysical interactions. *Biophys. Rev.* **13**, 259–272 (2021).
12. Scott, K. A. & Njardarson, J. T. Analysis of US FDA-Approved Drugs Containing Sulfur Atoms. *Top. Curr. Chem.* **376**, 5 (2018).
13. Mujumdar, P. & Poulsen, S.-A. Natural Product Primary Sulfonamides and Primary Sulfamates. *J. Nat. Prod.* **78**, 1470–1477 (2015).
14. Plunkett, S., Basch, C. H., Santana, S. O. & Watson, M. P. Harnessing Alkylpyridinium Salts as Electrophiles in Deaminative Alkyl–Alkyl Cross-Couplings. *J. Am. Chem. Soc.* **141**, 2257–2262 (2019).

15. Kiss, R., Sandor, M. & Szalai, F. A. http://Mcule.com: a public web service for drug discovery. *J. Cheminformatics* **4**, P17, 1758-2946-4-S1-P17 (2012). arthor.docking.org accessed 7/2/2024 for Mcule-BB-22Q1-2.1M (Smiles ID: [R]S(=O)(=O)N([H])[H] for aliphatic and aromatic primary sulfonamide; C(N([H])[H])[H] for aliphatic primary amine and C1(N([H])[H])=CC=CC=C1 for aniline, respectively).

16. Pedersen, P. S., Blakemore, D. C., Chinigo, G. M., Knauber, T. & MacMillan, D. W. C. One-Pot Synthesis of Sulfonamides from Unactivated Acids and Amines via Aromatic Decarboxylative Halosulfonylation. *J. Am. Chem. Soc.* **145**, 21189–21196 (2023).

17. Andrews, J. A. *et al.* Photocatalytic Carboxylate to Sulfinamide Switching Delivers a Divergent Synthesis of Sulfonamides and Sulfonimidamides. *J. Am. Chem. Soc.* **145**, 21623–21629 (2023).

18. Carson II, W. P., Sarver, P. J., Goudy, N. S. & MacMillan, D. W. C. Photoredox Catalysis-Enabled Sulfination of Alcohols and Bromides. *J. Am. Chem. Soc.* **145**, 20767–20774 (2023).

19. Li, Y., Xiao, F., Guo, Y. & Zeng, Y. Recent Developments in Deaminative Functionalization of Alkyl Amines. *Eur. J. Org. Chem.* **2021**, 1215–1228 (2021).

20. Berger, K. J. & Levin, M. D. Reframing primary alkyl amines as aliphatic building blocks. *Org. Biomol. Chem.* **19**, 11–36 (2021).

21. Kong, D., Moon, P. J. & Lundgren, R. J. Radical coupling from alkyl amines. *Nat. Catal.* **2**, 473–476 (2019).

22. Zhao, F. *et al.* Photocatalytic Hydrogen-Evolving Cross-Coupling of Arenes with Primary Amines. *Org. Lett.* **20**, 7753–7757 (2018).

23. Capperucci, A. & Tanini, D. Synthesis of Nitroarenes by Oxidation of Aryl Amines. *Chemistry* **4**, 77–97 (2022).

24. Andrews, J. A., Pantaine, L. R. E., Palmer, C. F., Poole, D. L. & Willis, M. C. Sulfinates from Amines: A Radical Approach to Alkyl Sulfonyl Derivatives via Donor–Acceptor Activation of Pyridinium Salts. *Org. Lett.* **23**, 8488–8493 (2021).

25. Barton, D. H. R., Bringman, G., Lamotte, G., Hay Motherwell, R. S. & Motherwell, W. B. Radical deamination reactions of relevance to aminoglycoside chemistry. *Tetrahedron Lett.* **20**, 2291–2294 (1979).

26. Wang, M., Fan, Q. & Jiang, X. Metal-free construction of primary sulfonamides through three diverse salts. *Green Chem.* **20**, 5469–5473 (2018).

27. Ashley, M. A. & Rovis, T. Photoredox-Catalyzed Deaminative Alkylation via C–N Bond Activation of Primary Amines. *J. Am. Chem. Soc.* **142**, 18310–18316 (2020).

28. Pincekova, L., Merot, A., Schäfer, G. & Willis, M. C. Sandmeyer Chlorosulfonylation of (Hetero)Aromatic Amines Using DABSO as an SO_2 Surrogate. *Org. Lett.* **26**, 5951−5955 (2020).

29. Kennedy, S. H., Dherange, B. D., Berger, K. J. & Levin, M. D. Skeletal editing through direct nitrogen deletion of secondary amines. *Nature* **593**, 223–227 (2021).

30. Masson-Makdissi, J. *et al.* Evidence for Dearomatizing Spirocyclization and Dynamic Effects in the Quasi-stereospecific Nitrogen Deletion of Tetrahydroisoquinolines. *J. Am. Chem. Soc.* **146**, 17719–17727 (2024).

31. Berger, K. J. *et al.* Direct Deamination of Primary Amines via Isodiazene Intermediates. *J. Am. Chem. Soc.* **143**, 17366–17373 (2021).

32. Dherange, B. D. *et al.* Direct Deaminative Functionalization. *J. Am. Chem. Soc.* **145**, 17–24 (2023).

33. Xue, J.-H., Li, Y., Liu, Y., Li, Q. & Wang, H. Site-Specific Deaminative Trifluoromethylation of Aliphatic Primary Amines. *Angew. Chem. Int. Ed.* **63**, e202319030 (2024).

34. Good, A. & Thynne, J. C. J. Reaction of free radicals with sulphur dioxide. Part 2.—Ethyl radicals. *Trans Faraday Soc* **63**, 2720–2727 (1967).

35. Sarver, P. J., Bissonnette, N. B. & MacMillan, D. W. C. Decatungstate-Catalyzed C(sp^3)–H Sulfinylation: Rapid Access to Diverse Organosulfur Functionality. *J. Am. Chem. Soc.* **143**, 9737–9743 (2021). In this study, MacMillan et al. were unable to identify transition states of methyl, primary, secondary, or tertiary radicals reacting with SO_2 using the (U)ωB97XD/6-31+G(d,p) set. Similarly, our attempts to scan along the C–S bond stretching resulted in a continuous increase in energy, indicating a very low barrier to radical addition across solvent conditions (see SI). These findings agree with experimentally observed low barriers to radical addition in unstabilized aliphatic radicals. However, the transition state calculations in the gas phase showed low barriers ($\Delta G^{\ddagger}$ = 7.5 and 6.8 kcal/mol for primary and secondary, respectively).

36. Graham, S. L. & Scholz, T. H. The Reaction of Sulfinic Acid Salts with Hydroxylamine-O-sulfonic Acid. A Useful Synthesis of Primary Sulfonamides. *Synthesis* **1986**, 1031–1032 (2002).

37. Emmett, E. J. & Willis, M. C. The Development and Application of Sulfur Dioxide Surrogates in Synthetic Organic Chemistry. *Asian J. Org. Chem.* **4**, 602–611 (2015).

38. You, T., Zhang, M., Chen, J., Liu, H. & Xia, Y. Ruthenium(II)-catalyzed reductive N–O bond cleavage of *N* -OR (R = H, alkyl, or acyl) substituted amides and sulfonamides. *Org. Chem. Front.* **8**, 112–119 (2021).

39. Denisenko, A. *et al.* 2-Oxabicyclo[2.1.1]hexanes as saturated bioisosteres of the ortho-substituted phenyl ring. *Nat. Chem.* **15**, 1155–1163 (2023).

40. Matošević, A. & Bosak, A. Carbamate group as structural motif in drugs: a review of carbamate derivatives used as therapeutic agents. *Arch. Ind. Hyg. Toxicol.* **71**, 285–299 (2020).

41. De, S. *et al.* Pyridine: the scaffolds with significant clinical diversity. *RSC Adv.* **12**, 15385–15406 (2022).

42. Digles, D. & Ecker, G. F. Self-Organizing Maps for In Silico Screening and Data Visualization. *Mol. Inform.* **30**, 838–846 (2011).

43. Maaten, L. van der & Hinton, G. Visualizing Data using t-SNE. *J. Mach. Learn. Res.* **9**, 2579–2605 (2008).

44. Visualizing Chemical Space, 2020. hhttps://github.com/PatWalters/workshop/blob/master/predictive_models/2_visualizing_chemical_space.ipynb (accessed March 14, 2023). *GitHub* https://github.com/PatWalters/workshop/blob/master/predictive_models/2_visualizing_chemical_space.ipynb.

45. Gualandi, A. *et al.* Photocatalytic Radical Alkylation of Electrophilic Olefins by Benzylic and Alkylic Zinc-Sulfinates. *ACS Catal.* **7**, 5357–5362 (2017).

46. Lewis, N. L. *et al.* Phase I Study of the Safety, Tolerability, and Pharmacokinetics of Oral CP-868,596, a Highly Specific Platelet-Derived Growth Factor Receptor Tyrosine Kinase Inhibitor in Patients With Advanced Cancers. *J. Clin. Oncol.* **27**, 5262–5269 (2009).

47. Galanis, A. *et al.* Crenolanib is a potent inhibitor of FLT3 with activity against resistance-conferring point mutants. *Blood* **123**, 94–100 (2014).

48. Smith, C. C. *et al.* Crenolanib is a selective type I pan-FLT3 inhibitor. *Proc. Natl. Acad. Sci.* **111**, 5319–5324 (2014).

49. Ecker, A. K., Levorse, D. A., Victor, D. A. & Mitcheltree, M. J. Bioisostere Effects on the EPSA of Common Permeability-Limiting Groups. *ACS Med. Chem. Lett.* **13**, 964–971 (2022).

50. Hirayama, F. *et al.* Design, synthesis and biological activity of YM-60828 derivatives: potent and orally-Bioavailable factor Xa inhibitors based on naphthoanilide and naphthalensulfonanilide templates. *Bioorg. Med. Chem.* **10**, 2597–2610 (2002).

51. Loudon, G. M., Radhakrishna, A. S., Almond, M. R., Blodgett, J. K. & Boutin, R. H. Conversion of aliphatic amides into amines with [I,I-bis(trifluoroacetoxy)iodo]benzene. 1. Scope of the reaction. *J. Org. Chem.* **49**, 4272–4276 (1984).

52. Evans, D.& Ripin, D. Evans pKa Table. ACS Organic Division, https://organicchemistrydata.org/hansreich/resources/pka/pka_data/evans_pKa_table.pdf (accessed 2024).

53. Neese, F., Hansen, A. & Liakos, D. G. Efficient and accurate approximations to the local coupled cluster singles doubles method using a truncated pair natural orbital basis. *J. Chem. Phys.* **131**, 064103 (2009).

54. Riplinger, C., Pinski, P., Becker, U., Valeev, E. F. & Neese, F. Sparse maps—A systematic infrastructure for reduced-scaling electronic structure methods. II. Linear scaling domain based pair natural orbital coupled cluster theory. *J. Chem. Phys.* **144**, 024109 (2016).